Am J Transl Res 2021;13(3):1257-1268
www.ajtr.org /ISSN:1943-8141/AJTR0124787

Original Article

Autologous transplantation of multilayered fibroblast sheets prevents postoperative pancreatic fistula by regulating fibrosis and angiogenesis

Keisuke Iwamoto[1], Toshiro Saito[1], Yoshihiro Takemoto[1], Koji Ueno[1], Masashi Yanagihara[1], Tomoko Furuya-Kondo[2], Hiroshi Kurazumi[1], Yuya Tanaka[1], Yohei Taura[1], Eijiro Harada[1], Kimikazu Hamano[1]

[1]Department of Surgery and Clinical Science, Yamaguchi University Graduate School of Medicine, Yamaguchi, Japan; [2]Department of Molecular Pathology, Yamaguchi University Graduate School of Medicine, Yamaguchi, Japan

Received October 22, 2020; Accepted January 11, 2021; Epub March 15, 2021; Published March 30, 2021

Abstract: Introduction: Postoperative pancreatic fistula (POPF) is a serious complication after gastrointestinal or pancreatic surgery. Despite intensive investigations, the occurrence has not significantly decreased in the past decades. The aims of this study were to clarify the pathophysiology of POPF and establish the preventive measures using multilayered fibroblast sheets. Methods: We developed a pancreatic fistula (PF) model of rat with transection of the splenic duct and surrounding pancreatic parenchyma. Multilayered fibroblast sheets prepared from tails were autologously transplanted to this model. The preventive effect was biochemically and histologically evaluated by measuring the ascitic levels of pancreatic enzymes and conducting immunohistochemistry and real-time polymerase chain reaction analyses of pancreatic tissue. Findings were compared to those obtained with acellular materials simply sealing the wound. Results: In the PF model, the ascitic levels of pancreatic enzymes were transiently up-regulated. Inflammation and necrosis were histologically observed in a wide range. Islets were damaged even in remote areas. Transplantation of multilayered fibroblast sheets dramatically reduced the ascitic leakage of enzymes, suppressed inflammation, and broadly preserved the islets. Compared with acellular materials, these sheets offered superior prevention of cellular activity through the spaciotemporal regulation of fibrosis and angiogenesis. Notably, the leakage hole appeared to have been plugged with the fibrotic matrix, which might have been the most crucial mechanism minimizing pancreatic damage. Conclusions: The autologous transplantation of multilayered fibroblast sheets significantly prevented PF and protected the pancreas, underscoring the potential utility of this approach for POPF prevention.

Keywords: Pancreatic fistula, autologous transplantation, multilayered fibroblast sheets, fibrosis, angiogenesis

Introduction

Postoperative pancreatic fistula (POPF) is a serious complication after gastrointestinal or pancreatic surgery, characterized by the leakage of digestive enzymes that causes tissue injury and life-threatening sequelae. The leakage from an exfoliated surface and anastomotic stump is believed to be the primary cause of POPF. Despite numerous reports describing the prediction or prevention of POPF, its occurrence has not significantly decreased over the last three decades [1]. Accordingly, the development of POPF preventive measures is urgently required. However, an ideal strategy has yet to be established.

Thus far, fibrin sealants, bioabsorbable mesh, stents and anastomotic techniques have been developed [2-7]. These techniques buttress the mechanical stress or reinforce the anastomosis, but they've shown only a marginal salutary effect. In addition to the loss of mechanical integrity, other mechanisms may underlie the pathophysiology of POPF. In fact, recent evidence suggests the involvement of postoperative pancreatitis and ischemia [8-10]. A basic/translational study that clarifies the multifactorial mechanisms involved in POPF should be conducted.

In previous studies, regenerative medicine was applied to animal models in an attempt to pre-

vent POPF [11-13]. The transplantation of cell sheets with myoblasts, adipose-derived stem cells or mesenchymal stem cells to pancreatic fistula (PF) models of rat successfully demonstrated the therapeutic utility of such approaches. However, while the transplantation of cell sheets is considered a promising approach, the preparation of stem cells takes a substantial amount of time and is costly, which may limit its clinical application. It is therefore important to optimize the cell sheets, especially in their handling and preparation.

Interestingly, recent evidence in regenerative medicine has suggested that the functional recovery in recipient organs is primarily mediated through endogenous regeneration stimulated by the transplant rather than through the direct differentiation of exogenous stem cells into functional tissue [14-16]. While the differentiation of stem cells has hardly been documented *in vivo*, the secreted factors from the transplant, including growth factor and miRNA, provoke endogenous angiogenesis, cell proliferation and migration, thereby significantly contributing to functional restoration [14-16]. Since non-stem cells are also capable of secreting these factors, their transplantation could be applicable in a context-dependent manner. Indeed, the closure of a fistula may be important for POPF prevention as well as islet regeneration. Attempting to transplant non-stem cells for the wound healing in PF models therefore seems to have some merit. To this end, we previously developed multilayered fibroblast sheets in rodents and demonstrated effective wound healing with their transplantation to refractory skin ulcers in an animal model [17].

The present study thus aimed to clarify whether or not the autologous transplantation of multilayered fibroblast sheets prevents PF in a rat model. Our investigations were initiated with the pathophysiological analysis of a PF model. We uncovered chronological changes in inflammation and fibrosis, i.e. a previously undescribed nature of pancreatic remodeling in this model. We subsequently examined the effects of their autologous transplantation to our PF model and found significant prevention. Compared with non-viable material, the cellular activity of these sheets allowed for the temporal and spatial regulation of fibrosis, restricting inflammation and preserving the islets. Angiogenesis, a critical factor for tissue recovery, was also induced by these sheets. As a result, the present study showed, for the first time, that autologous transplantation of multilayered fibroblast sheets prevents PF and protects the pancreas from pathological remodeling using a rat model.

Materials and methods

Animals

Male Wistar and SD rats (10-12 weeks old), and male SD-Tg (CAG-eGFP) rats (7 weeks old) were purchased from Japan SLC (Shizuoka, Japan). They were housed in a temperature-, humidity-, and light-controlled room (12 h light/dark cycles) with *ad libitum* access to food and water. This study was approved by the Institutional Animal Care and Use Committee of Yamaguchi University (IACUC; No. 31-005).

Preparation of cell sheets

The detailed protocol was described as previously [17]. In brief, fibroblasts were isolated from the tail of rat using collagenase (Wako, Osaka, Japan) and cultured with CTSTM AIM V® medium (Thermo Fisher Scientific, Waltham, MA, USA) supplemented with 10% fetal bovine serum (FBS) in an incubator at 37°C. The fibroblasts at confluence were detached and incubated at a concentration of 2.0×10^5 cells/ml. A 2-ml mixture was seeded into each well of 24-well plates. After 2-day culture, multilayered fibroblasts were detached from the plate with 10 PU/ml Dispase (Wako) and a viable sheet was obtained. By subjecting the viable sheet to three freeze-thaw cycles, a non-viable sheet was obtained. The loss of cellular viability was confirmed with Cell Count Reagent SF (NACALAI TESQUE, Kyoto, Japan).

PF model and transplantation of cell sheets

The rats were randomly divided into four groups: a laparotomy (sham) group, pancreatic resection (PF) group, pancreatic resection patched with multilayered fibroblast sheets (viable sheet) group and non-viable sheet group. The sham group underwent laparotomy with only a 5-cm incision along the midline of the abdomen. The rat pancreatic ducts consist of 4 ducts, e.g. common duct, gastric duct, duodenal duct, and splenic duct (Supplementary

Table 1. Primer sequences

	Forward	Reverse
Collagen type I α I	TACAGCACGCTTGTGGATGG	GGGAGGTCTTGGTGGTTTTG
Collagen type III α I	GGCAGGGAACAACTGATGG	GGGTGAAGCAGGGTGAGAAG
Vegf α	GGGCCTCTGAACCCATGAAC	CATGGTGGAGGTACAGCAGTAAAG
Tgf β I	GATACGCCTGAGTGGCTGTC	AAGCCCTGTATTCCGTCTCC
Tubulin α I α	CCTACCCTCGCATCCACTTC	GCAGGCATTGGTGATCTCTG

Primer sequences for real-time PCR are listed.

Figure 1). The PF group underwent transection of the splenic duct and surrounding pancreatic parenchyma with the preservation of the splenic artery and vein. The viable sheet and non-viable sheet groups underwent transplantation of multilayered fibroblast sheets and non-viable sheets, respectively, to the transection of the pancreas. Rats were sacrificed on day 1 or 3 after the operation. At relaparotomy, the abdominal cavity was rinsed with 1 ml saline, and ascites was collected for the measurement of amylase and lipase content. Blood and pancreatic tissue were also collected. The ascites and blood were centrifuged at 3000 rpm for 20 minutes to remove debris. The samples were stored at 4°C or -80°C.

Analyses of pancreatic enzymes in ascites and serum

We commissioned the measurements of amylase and lipase from SRL (Tokyo, Japan). These values were measured using standard laboratory methods [11].

Histological analyses

The detailed protocol was described previously [17]. In brief, rat pancreatic tissues were immediately fixed with 10% Formalin Neutral Buffer Solution (Wako). The samples were then dehydrated in a grade ethanol series of washes and embedded in paraffin. Three-micrometer-thick sections were mounted on glass slides and stained with hematoxylin and eosin (HE) or Masson's trichrome (MT). Immunostaining was performed using primary for GFP (#2956, Cell Signaling Technology, Danvers, MA, USA) and von Willebrand Factor (#65707, Cell Signaling Technology) and secondary antibodies for Goat Anti-Rabbit IgG H&L (FITC) (ab97050, Abcam, Cambridge, UK), Goat anti-Mouse IgG (H+L) Cross-Absorbed Secondary Antibody, Alexa Fluor 555 (Thermo Fisher Scientific) and Goat Anti-Rabbit IgG H&L (DyLight® 550) (ab96-884, Abcam) in accordance with the manufacturer's instruction. Pathologists examined the HE and MT stains.

Quantification of angiogenesis

To assess the angiogenesis, 10 fields (high-power field, × 40) were randomly selected from each rat pancreatic tissue. The number of small tube structure labelled with vWF antibody was manually counted.

Real-time polymerase chain reaction (PCR) analyses

The detailed protocol was described previously [18]. In brief, total RNA was extracted from the pancreas using RNase Mini Kit (Qiagen, Hilden, Germany). cDNA was synthesized using 15 ng of total RNA and PrimeScript Reverse Transcription (Takara Bio, Shiga, Japan). To compare the mRNA expression, the reverse transcription product was then subjected to real-time PCR with SYBR Select Master Mix (Thermo Fisher Scientific) using StepOnePlus (Thermo Fisher Scientific). Primer sequences are listed in the **Table 1**.

Statistical analyses

The data are expressed as the mean ± standard error of the mean of the indicated number of experiments or rats. Either the Tukey-Kramer test or Student's *t*-test was used to determine the statistical significance. A value of $P<0.05$ was considered to be statistically significant.

Results

Production of PF model

Based on previous reports [11-13], we engineered a rat PF model with transection of the splenic duct and surrounding pancreatic parenchyma (Supplementary Figure 1). As a macroscopic finding, swelling and reddening was apparent in the peritoneal organs in the PF model compared to the control animals (sham) (Supplementary Figure 2A-F). The inflammation and ascites were more prominent on postoper-

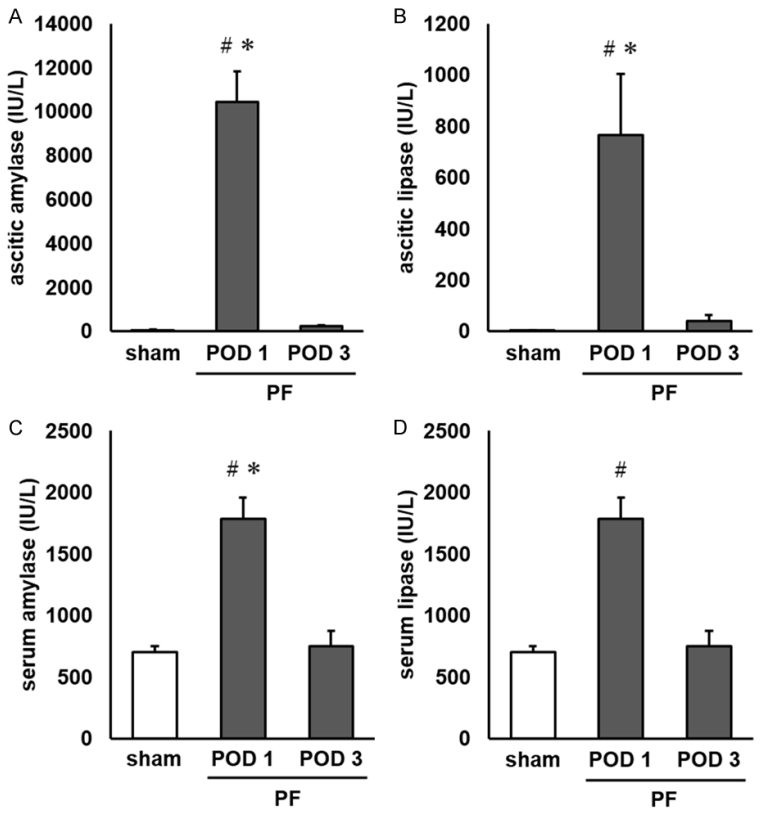

Figure 1. Biochemical analyses of the pancreatic fistula (PF) model. Ascitic and serum levels of amylase and lipase were assessed in the sham and the PF models on postoperative day (POD) 1 and 3. The levels of ascitic amylase (A), ascitic lipase (B), serum amylase (C) and serum lipase (D) are summarized (n=7 per group). The error bar represents the SEM. #*P*<0.01 versus sham, **P*<0.01 versus POD 3 (Tukey Kramer test).

ative day (POD) 1 than on POD 3 (Supplementary Figure 2C-F). Biochemically, the ascitic levels of amylase and lipase were transiently up-regulated with a peak at POD 1, suggesting the acute leakage of pancreatic enzymes (**Figure 1A** and **1B**). The serum levels of these enzymes similarly showed transient elevation (**Figure 1C** and **1D**). Thus, the successful reproduction of the PF model reported by other investigators was achieved.

On POD 1, the infiltration of neutrophils was histologically observed in a wide range in the PF model compared to the sham model (**Figure 2A** and **2B**, arrows), and islets had almost disappeared around the transection site, accompanied by necrosis (**Figure 2B**, arrowheads). On POD 3, the infiltration of fibroblasts, collagen deposition and granulation were observed (**Figure 2C**, arrows). Of note, the atrophy of islets was present even in the remote area (**Figure 2B** and **2C**, arrowheads), suggesting the expansion of inflammation and pancreatitis.

Salutary effects of fibroblast sheets transplanted to PF model

To prevent PF, we patched a multilayered fibroblast sheets (viable sheet) around the transection site shortly after the transection of the splenic duct and surrounding pancreatic parenchyma. These sheets successfully suppressed inflammation as a macroscopic finding (Supplementary Figure 3). The ascitic levels of pancreatic enzymes were significantly reduced in the sheet group compared to the PF model (**Figure 3A** and **3B**). The serum levels of enzymes were also down-regulated in response to sheet therapy (**Figure 3C** and **3D**), suggesting the suppression of pancreatitis. Interestingly, fibrosis was regionally and intensively observed just around the transection, as early as on POD 1, in the sheet group (**Figure 4A**, arrows). A leakage hole appeared to be plugged with fibrotic extracellular matrix. The necrotic area was restricted, and the normal structure of the islet was largely preserved in response to sheet therapy (**Figure 4A** and **4B**, arrowheads). The maturation of fibrosis appeared on POD 3 (**Figure 4B**, arrows). These results clearly demonstrated the salutary effect of multilayered fibroblast sheets (viable sheet) in preventing PF and protecting the pancreas.

Several questions were raised regarding the mechanism by which this viable sheet effectively prevented PF. Given that acellular nonviable materials are clinically used to prevent PF [2-4, 19, 20], we wondered: (1) whether or not the physical sealing of the transection site was critical, and (2) whether or not the cellular activity of the fibroblast sheets was important.

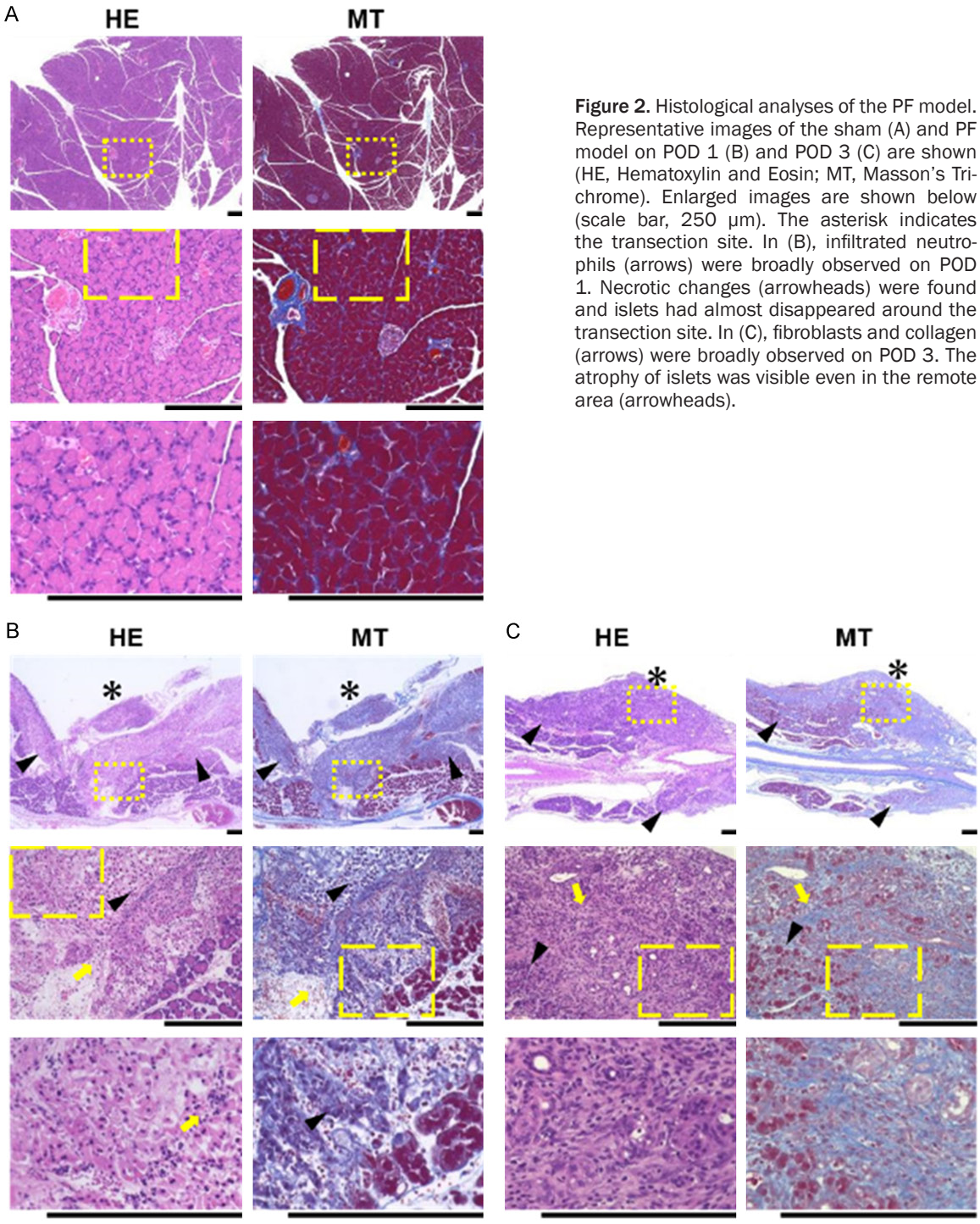

Figure 2. Histological analyses of the PF model. Representative images of the sham (A) and PF model on POD 1 (B) and POD 3 (C) are shown (HE, Hematoxylin and Eosin; MT, Masson's Trichrome). Enlarged images are shown below (scale bar, 250 μm). The asterisk indicates the transection site. In (B), infiltrated neutrophils (arrows) were broadly observed on POD 1. Necrotic changes (arrowheads) were found and islets had almost disappeared around the transection site. In (C), fibroblasts and collagen (arrows) were broadly observed on POD 3. The atrophy of islets was visible even in the remote area (arrowheads).

To address these questions, we used acellular materials to patch the transection in a PF model and compared its preventive effect to that obtained with multilayered fibroblast sheets. Since rat pancreas is thin and tiny, there were only a few candidate acellular materials that were light and thin enough for transplantation to this small organ. One candidate was the multilayered cytoskeleton sheets created by repeated freezing and thawing of the multilayered fibroblast sheets. We confirmed the loss of cellular viability in these sheets (Supplementary Figure 4). Another was Seprafilm, which is used in clinical surgery as a bioabsorbable

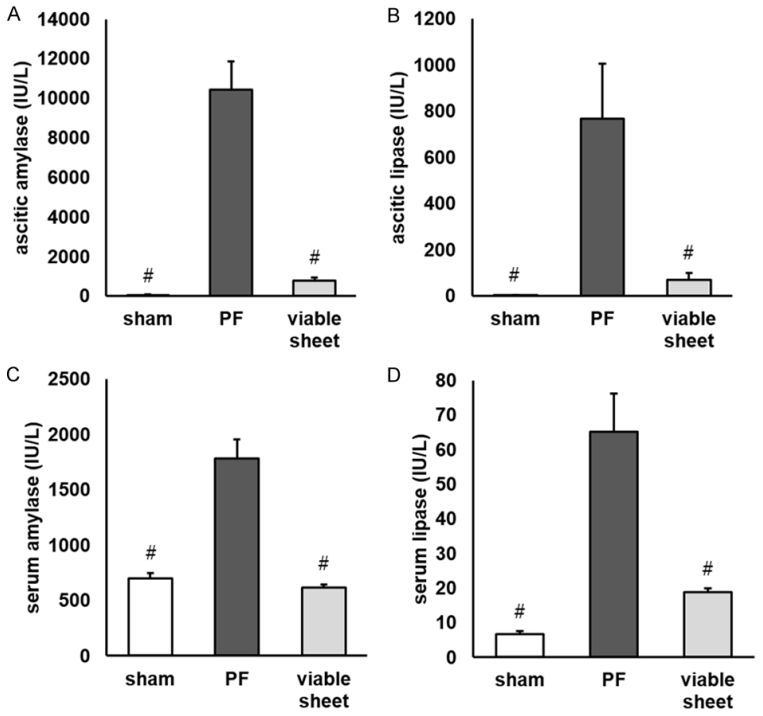

Figure 3. Biochemical analyses show that the autologous transplantation of multilayered fibroblast sheets (viable sheet) significantly prevents PF. The ascitic and serum levels of amylase and lipase were assessed in the sham, PF and viable sheet groups on POD 1. The levels of ascitic amylase (A), ascitic lipase (B), serum amylase (C) and serum lipase (D) are summarized (n=7 per group). The error bar represents the SEM. #P<0.01 versus PF group (Tukey Kramer test).

material consisting of sodium hyaluronate and carboxymethylcellulose. These materials successfully reduced the ascitic levels of pancreatic enzymes to a similar extent (The data obtained with Seprafilm are not shown). However, the preventive effect obtained with non-viable sheet was significantly inferior to that with the multilayered fibroblast sheets (viable sheet) (**Table 2**). Similar results were obtained with regard to the serum levels of pancreatic enzymes (**Table 2**). Consistently, histological analyses showed that the acellular materials only partially suppressed the necrosis and rescued fewer islets than the multilayered fibroblast sheets (Supplementary Figure 5). Regional and intensive fibrosis was absent in response to acellular materials. These results suggest that the physical sealing with acellular materials prevents PF to some extent, but the viable sheet provides a further salutary effect.

Given that multilayered fibroblast sheets prepared from the tails of mice provoke angiogenesis by secreting various growth factors, e.g. vascular endothelial growth factor (VEGF) and hepatocyte growth factor (HGF) [17, 21], we speculated that angiogenesis might be induced in the pancreas treated with the viable sheet. Based on the finding by pathologists that the ring structures compatible with small vessels were observed only in the viable sheet group and not in the non-viable sheet group on HE and MT stains of pancreatic tissue, we evaluated angiogenesis via immunohistochemistry with antibody to von Willebrand Factor (vWF), a vascular endothelial marker. Although there was no remarkable difference in angiogenesis between the viable sheet and non-viable sheet groups on POD1, small vessels labelled with anti-vWF antibody were found around the transection site only in the viable sheet group on POD 3 (**Figure 5**), suggesting that the viable sheet induced angiogenesis in the sub-acute phase.

Viability of fibroblast sheets

In order to evaluate how long the transplanted sheets maintained the cellular activity *in vivo*, we used a transgenic rat ubiquitously expressing enhanced green fluorescent protein (eGFP). After the transplantation of multilayered fibroblast sheets prepared from Tg (CAG-eGFP)-rat to the PF model of non-Tg (NTg)-rat, GFP signal was broadly observed around the transection on POD 1 (**Figure 6A**); however, the signal was almost lost on POD 3 (**Figure 6B**). This result suggests that the transplanted sheets are viable on POD 1 and their cellular activity does not last for more than three days. We hypothesized that these sheets were exposed to digestive enzymes without sufficient nutrients, thereby losing their viability within a short period of time. In order to test the hypothesis, we conducted an *in vitro* experiment mimicking the transplanted sheets in a PF model. We evaluated the viability of cultured fibroblasts in the presence or absence of artificial intestinal juice

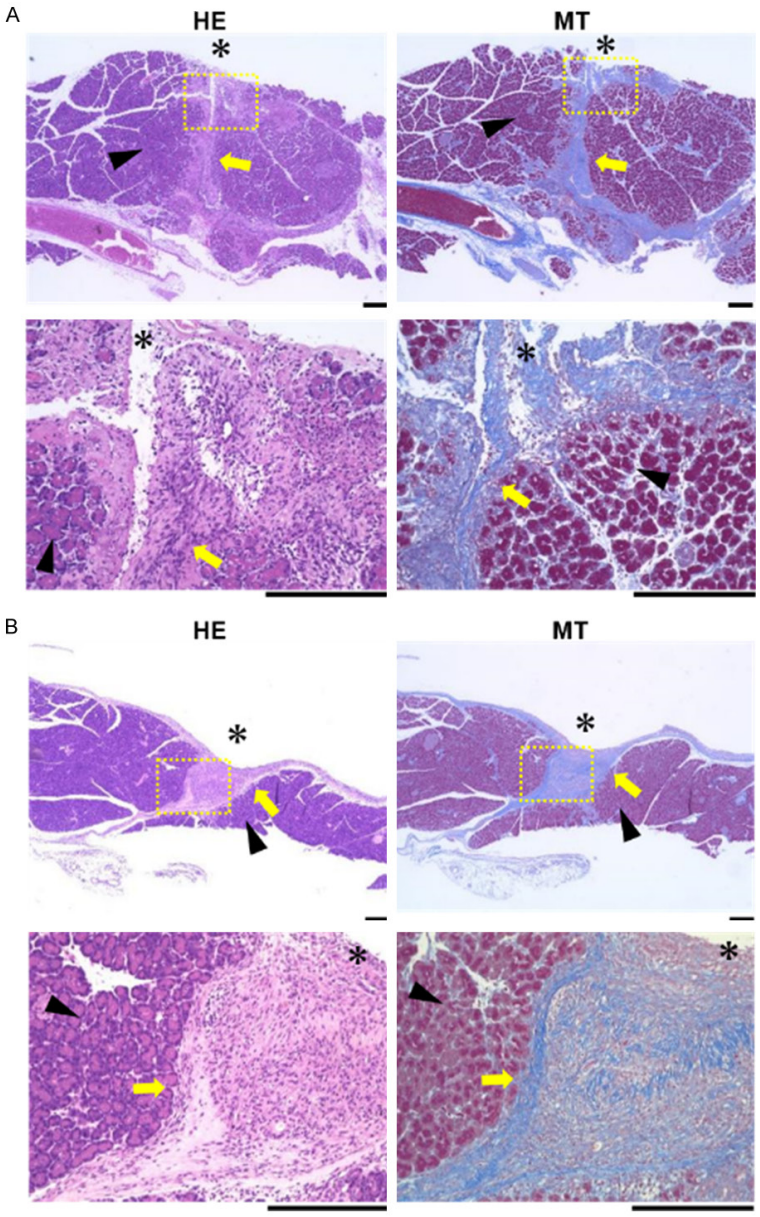

Figure 4. Histological analyses demonstrate that the autologous transplantation of multilayered fibroblast sheets (viable sheet) significantly prevents PF. Representative images of the viable sheet group on POD 1 (A) and POD 3 (B) are shown (HE, Hematoxylin and Eosin; MT, Masson's Trichrome). Enlarged images are shown below (scale bar, 200 μm). The asterisk indicates the transection site. In (A), regional and intensive fibrosis (arrows) was observed just around the transection on POD 1. The preserved islets (arrowheads) were broadly found, even close proximity to the transection site. In (B), matured fibrosis (arrows) and preserved islets (arrowheads) were observed on POD 3.

and nutrients. As expected, the viability of the cultured fibroblasts was seriously impaired in the presence of artificial intestinal juice or the absence of sufficient nutrients (Supplementary Figure 6). These results suggest that the multilayered fibroblast sheets remain viable only in the acute phase, although they nevertheless successfully exert a salutary effect.

Analyses of mRNA expression in the pancreas treated with fibroblast sheets

We analyzed the transcript levels of genes of interest. In the PF model and non-viable sheet group, the expression of *Collagen 1a* was very low and not obviously changed on POD 1 compared to that in the sham group, after which an upward trend was shown on POD 3 (**Figure 7A**). This result is consistent with the histological change showing the infiltration of fibroblasts on POD 3 in the PF model (**Figure 2B**). In the viable sheet group, an extremely high level of *Collagen 1a* was observed as early as POD 1 (**Figure 7A**). Since the viable sheet maintained its cellular activity on POD 1 (**Figure 6A**), the high level of *Collagen 1a* on POD 1 might be attributed to the transplanted fibroblasts. A similar trend was observed regarding the transcription of *Collagen 3a* (**Figure 7B**). These results are consistent with the histological change showing the earlier induction of fibrosis on POD 1 in a viable sheet group than the PF model (**Figures 2B** and **4A**). Interestingly, the analysis of *Vegf-α* and *Tgf-β* showed a different tendency. Although there was no statistical significance, an upward trend in the expression of *Vegf-α* and *Tgf-β* was observed on POD 3 only in the viable sheet group (**Figure 7C** and **7D**). Since the transplant lost viability on POD 3, this trend might reflect the activation of endogenous tissues, which may accelerate subsequent wound healing.

Table 2. Multilayered fibroblast sheets (viable sheet) are superior to acellular materials in preventing PF

	viable sheet group (n=7)	non-viable sheet group (n=7)	*p* value
Ascitic amylase (IU/L)	766.6 ± 181.4	2170.3 ± 531.6	0.039
Ascitic lipase (IU/L)	68.7 ± 32.1	246.3 ± 72.1	0.071
Serum amylase (IU/L)	620.4 ± 27.3	724.7 ± 35.4	0.039
Serum lipase (IU/L)	18.7 ± 1.7	25.9 ± 3.2	0.053

Unpaired Student's t-test. The ascitic and serum levels of amylase and lipase were assessed in the non-viable sheet group on POD 1 and compared to the viable sheet group. The levels of ascitic amylase, ascitic lipase, serum amylase and serum lipase are summarized. The ascitic and serum levels of amylase were significantly lower in the viable sheet group than those in the non-viable sheet group. The data are expressed as mean ± SEM.

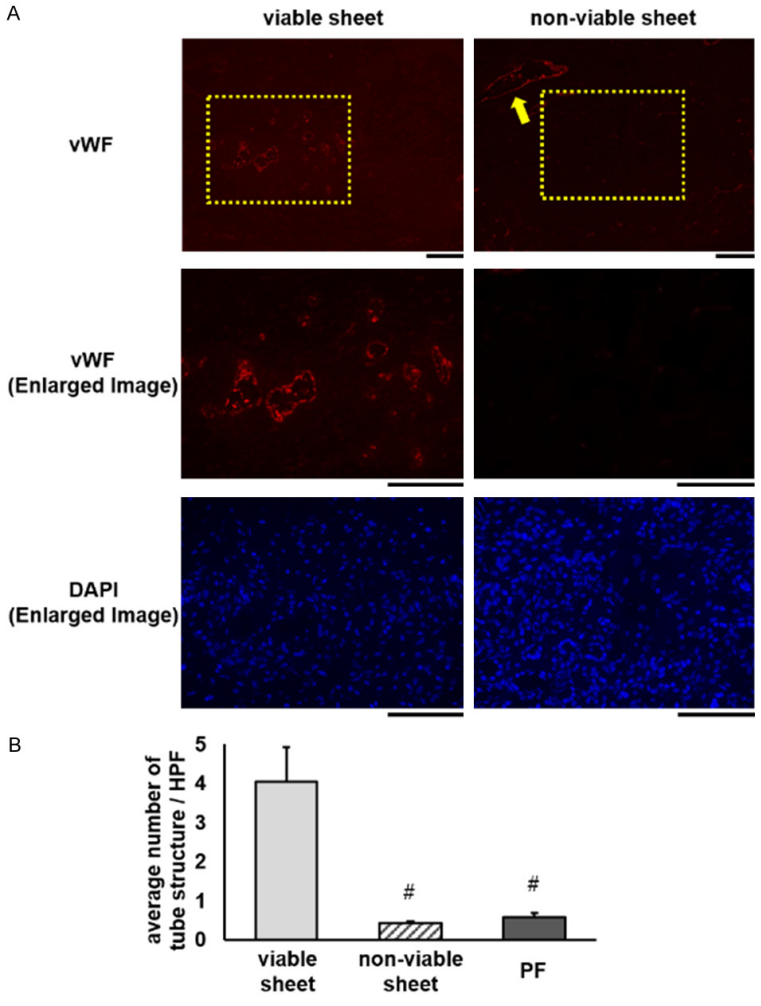

Figure 5. Multilayered fibroblast sheets (viable sheet), not non-viable sheets, induce angiogenesis. A. Representative images of von Willebrand Factor (vWF) and DAPI stains are shown. The viable sheet and non-viable sheet group were assessed on POD 3. The demarcation indicates the area shown under higher magnification (scale bar, 100 μm). In viable sheet group, the vWF signals showed ring structures compatible with small vasculature around the transection site, suggesting angiogenesis in response to the viable sheet. In non-viable sheet group, large vessels (arrow) were successfully stained, but the signals representing small vasculatures were absent. B. The number of tube structure labelled with vWF was assessed in PF, viable sheet and non-viable sheet group on POD 3 (n=3 per group). The error bar represents the SEM. #*P*<0.01 versus the viable sheet group (Tukey Kramer test).

Discussion

In the present study, we showed for the first time that autologous transplantation of multilayered fibroblast sheets significantly prevents PF and broadly preserves the islets in a rat model of PF. The cellular activity of these sheets induced well-controlled fibrosis and angiogenesis and protected the pancreas. We believe that our study provides the significant insight into the pancreatic pathophysiology and surgical methodology.

This study has at least two novel findings. First, chronological changes in pancreatic remodeling in a PF model were documented. Thus far, mouse models of acute and chronic pancreatitis in numerous studies have helped improve our understanding of their pathophysiology [22, 23]. However, no mouse models of POPF are available at present, and there is a paucity of studies examining the precise mechanisms involved [1, 8]. Since the rat pancreas is small, our PF model failed to reproduce many aspects of human clinical POPF; nonetheless, the present study may help further our understanding of the multifactorial mechanisms involved in POPF.

On POD 1, inflammatory cells showed wide infiltration. Due to the harsh damage that had

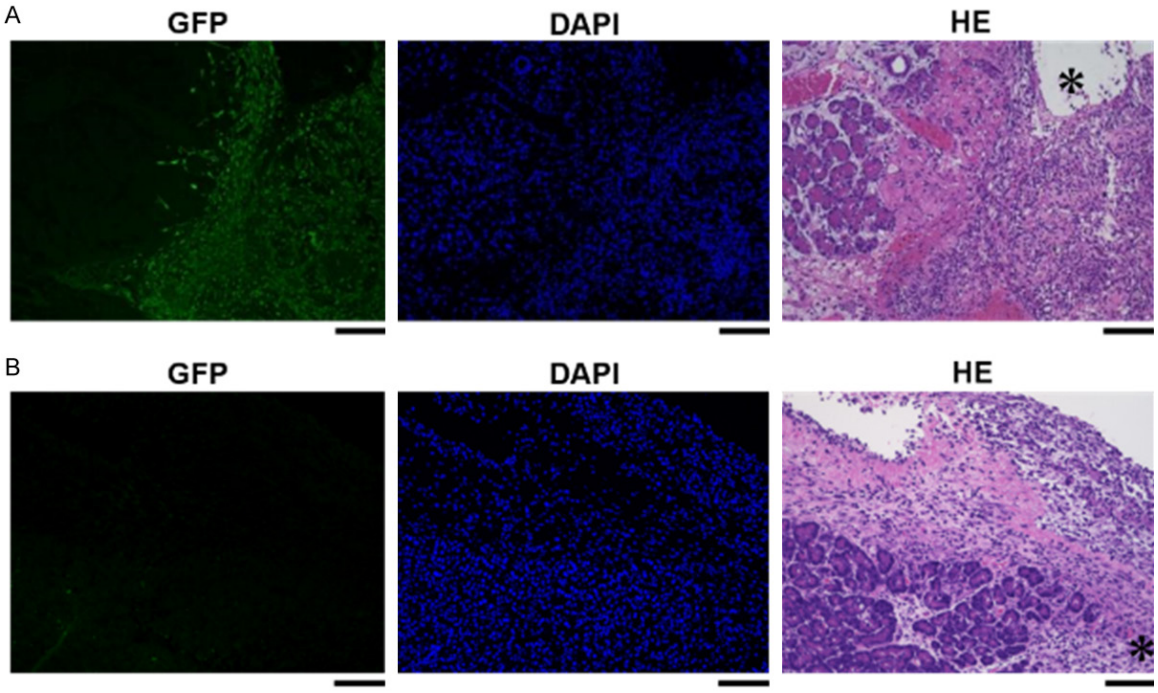

Figure 6. The viability of multilayered fibroblast sheets. The viability of multilayered fibroblast sheets was assessed on POD 1 (A) and on POD 3 (B). The sheets prepared from Tg (CAG-eGFP)-rat were transplanted to the PF model of non-Tg (NTg)-rat. The pancreatic tissue was analyzed with immunohistochemistry. Representative images of GFP, DAPI and Hematoxylin and Eosin (HE) stains on POD 1 are shown (scale bar, 100 μm). The asterisk indicates the transection site.

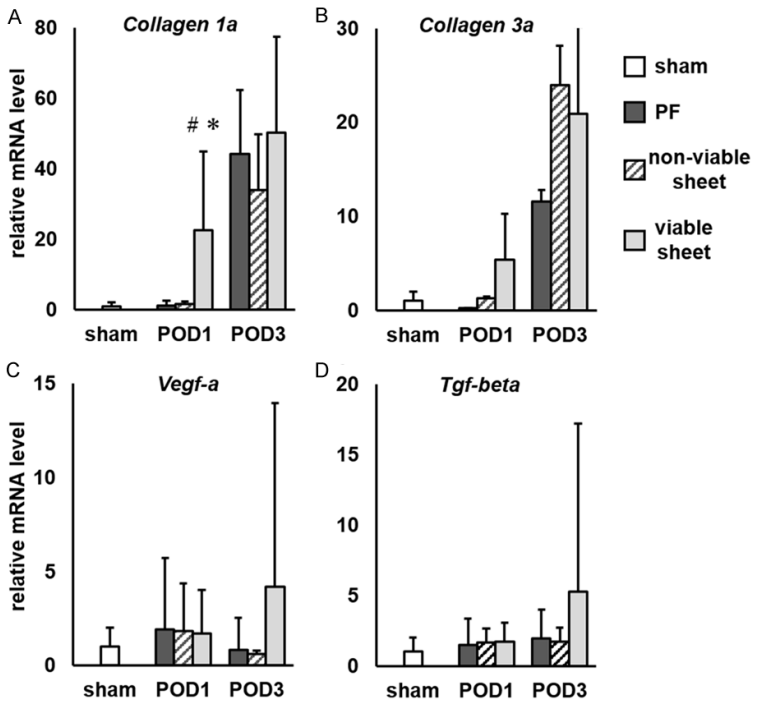

Figure 7. Multilayered fibroblast sheets (viable sheets) provoke the fibrosis and angiogenesis through direct and indirect (paracrine) mechanism. The mRNA levels of indicated genes were assessed by real-time PCR. The expression levels of *Collagen 1a* (A), *Collagen 3a* (B), *Vegf-α* (C), *Tgf-β* (D) are summarized (n=4 per group). The error bar represents the SEM. #P<0.05 versus the PF group on POD 1, *P<0.05 versus the non-viable sheet group on POD 1 (unpaired Student's t test).

been inflicted, the islets around the transection site had almost disappeared accompanied by necrotic changes. On POD 3, the infiltration of fibroblasts, collagen deposition and granulation were observed. Due to the inflammation, the atrophy of islets was noted even in remote areas. These histological changes were consistent with the data obtained via biochemical analyses. Although human clinical studies have suggested that postoperative pancreatitis and ischemia are involved in the development of POPF [1, 9, 10], in-depth histological and biochemical analyses are very limit-

ed. The present study thus helps further our understanding of POPF mechanisms.

Another novelty is the therapeutic potential of multilayered fibroblast sheets. We found that these sheets exerted significantly more cellular activity than non-viable materials, which allowed for intensive fibrosis to plug the leakage hole in the acute phase. This temporal and spatial control of fibrosis might be the most crucial mechanism minimizing the pancreatic damage. By restricting the inflammation in the acute phase, the islets in the remote area were well-preserved, i.e. pathological remodeling was suppressed. In human studies, softness and low interlobular fibrosis are considered risk factors for the POPF development [24, 25]. Targeting fibrosis may be a potential strategy against it. In addition, we found that angiogenesis was induced in response to the transplantation of this sheet on POD 3. Given that this sheet secrets an abundant amount of growth factors [17, 21], it is conceivable that endogenous angiogenesis was stimulated in the damaged pancreas in a paracrine manner, which would be crucial for the functional restoration thereafter.

Recently we found that the fibroblast sheets maintain a relatively substantial amount of cellular activity, such as the secretion of growth factors, after a single cycle of freezing and thawing (unpublished data). The autologous transplantation of human fibroblast sheets, whether fresh or after the thawing of frozen stock, may be a potential strategy for managing patients at a high risk of POPF who are scheduled to undergo surgery.

Several limitations associated with the present study warrant mention. First, our PF model showed the transient elevation of ascitic levels of pancreatic enzymes on POD 1; however, the leakage was reduced on POD 3 despite no intervention, suggesting that this model does not resemble serious POPF observed in human patients. Second, our multilayered fibroblast sheets failed to retain viability beyond POD 3 *in vivo*. Due to their short life, these sheets may not be useful for preventing prolonged or late-onset POPF. Further attempts should be made to improve the viability of this sheet against digestive enzymes. Third, there was marked variance in the characteristics of the rat pancreases, e.g. size and fat content, which made it technically difficult to create a homogeneous PF model; this might have caused large variance in some analyses.

In conclusion, the present study demonstrated the preventive potential of multilayered fibroblast sheets transplanted to a PF model. The cellular activity of these sheets allows for well-controlled fibrosis and angiogenesis and protects the damaged pancreas. Further investigations regarding the viability or functionality of the fibroblast sheets will be required for large animal studies or human clinical trials.

Acknowledgements

We thank Yukari Hironaka for technical support and Dr. Brian Quinn for linguistic comments and help with the article. This work was supported in part by Grants-in-Aids for Scientific Research (B) (19H03739 to K.H.) and Young Scientists (19K17601 to T.S.) from the Japan Society for the Promotion of Science; and grants from MSD Life Science Foundation, Public Interest Incorporated Foundation; Cardiovascular Research Fund; The Ichiro Kanehara Foundation for the Promotion of Medical Sciences and Medical care; and The Mochida Memorial Foundation for Medical and Pharmaceutical Research.

Disclosure of conflict of interest

None.

Address correspondence to: Dr. Toshiro Saito, Department of Surgery and Clinical Science, Yamaguchi University Graduate School of Medicine, 1-1-1 Minami-Kogushi, Ube, Yamaguchi 755-8505, Japan. Tel: +81-836-22-2260; Fax: +81-836-22-2262; E-mail: saitot@yamaguchi-u.ac.jp

References

[1] Nahm CB, Connor SJ, Samra JS and Mittal A. Postoperative pancreatic fistula: a review of traditional and emerging concepts. Clin Exp Gastroenterol 2018; 11: 105-118.

[2] Deng Y, He S, Cheng Y, Cheng N, Gong J, Gong J, Zeng Z and Zhao L. Fibrin sealants for the prevention of postoperative pancreatic fistula following pancreatic surgery. Cochrane Database Syst Rev 2020; 3: CD009621.

[3] Weniger M, D'Haese JG, Crispin A, Angele MK, Werner J and Hartwig W. Autologous but not fibrin sealant patches for stump coverage reduce clinically relevant pancreatic fistula in

distal pancreatectomy: a systematic review and meta-analysis. World J Surg 2016; 40: 2771-2781.
[4] Yamamoto M, Hayashi MS, Nguyen NT, Nguyen TD, McCloud S and Imagawa DK. Use of seamguard to prevent pancreatic leak following distal pancreatectomy. Arch Surg 2009; 144: 894-899.
[5] Jang JY, Chang YR, Kim SW, Choi SH, Park SJ, Lee SE, Lim CS, Kang MJ, Lee H and Heo JS. Randomized multicentre trial comparing external and internal pancreatic stenting during pancreaticoduodenectomy. Br J Surg 2016; 103: 668-675.
[6] Kitahata Y, Kawai M and Yamaue H. Clinical trials to reduce pancreatic fistula after pancreatic surgery-review of randomized controlled trials. Transl Gastroenterol Hepatol 2016; 1: 4.
[7] Chikhladze S, Makowiec F, Küsters S, Riediger H, Sick O, Fichtner-Feigl S, Hopt UT and Wittel UA. The rate of postoperative pancreatic fistula after distal pancreatectomy is independent of the pancreatic stump closure technique - a retrospective analysis of 284 cases. Asian J Surg 2020; 43: 227-233.
[8] Bannone E, Andrianello S, Marchegiani G, Masini G, Malleo G, Bassi C and Salvia R. Postoperative acute pancreatitis following pancreaticoduodenectomy: a determinant of fistula potentially driven by the intraoperative fluid management. Ann Surg 2018; 268: 815-822.
[9] Raty S, Sand J and Nordback I. Detection of postoperative pancreatitis after pancreatic surgery by urine trypsinogen strip test. Br J Surg 2007; 94: 64-69.
[10] Ansorge C, Regner S, Segersvard R and Strommer L. Early intraperitoneal metabolic changes and protease activation as indicators of pancreatic fistula after pancreaticoduodenectomy. Br J Surg 2012; 99: 104-111.
[11] Kaneko H, Kokuryo T, Yokoyama Y, Yamaguchi J, Yamamoto T, Shibata R, Gotoh M, Murohara T, Ito A and Nagino M. Novel therapy for pancreatic fistula using adipose-derived stem cell sheets treated with mannose. Surgery 2017; 161: 1561-1569.
[12] Kim SR, Yi HJ, Lee YN, Park JY, Hoffman RM, Okano T, Shim IK and Kim SC. Engineered mesenchymal stem-cell-sheets patches prevents postoperative pancreatic leakage in a rat model. Sci Rep 2018; 8: 360.
[13] Tanaka T, Kuroki T, Adachi T, Ono S, Kitasato A, Hirabaru M, Takatsuki M and Eguchi S. Development of a novel rat model with pancreatic fistula and the prevention of this complication using tissue-engineered myoblast sheets. J Gastroenterol 2013; 48: 1081-1089.
[14] Mazini L, Rochette L, Admou B, Amal S and Malka G. Hopes and limits of adipose-derived stem cells (ADSCs) and mesenchymal stem cells (MSCs) in wound healing. Int J Mol Sci 2020; 21: 1306.
[15] Shudo Y, Miyagawa S, Ohkura H, Fukushima S, Saito A, Shiozaki M, Kawaguchi N, Matsuura N, Shimizu T, Okano T, Matsuyama A and Sawa Y. Addition of mesenchymal stem cells enhances the therapeutic effects of skeletal myoblast cell-sheet transplantation in a rat ischemic cardiomyopathy model. Tissue Eng Part A 2014; 20: 728-739.
[16] Miyagawa S, Domae K, Yoshikawa Y, Fukushima S, Nakamura T, Saito A, Sakata Y, Hamada S, Toda K, Pak K, Takeuchi M and Sawa Y. Phase I clinical trial of autologous stem cell-sheet transplantation therapy for treating cardiomyopathy. J Am Heart Assoc 2017; 6: e003918.
[17] Mizoguchi T, Ueno K, Takeuchi Y, Samura M, Suzuki R, Murata T, Hosoyama T, Morikage N and Hamano K. Treatment of cutaneous ulcers with multilayered mixed sheets of autologous fibroblasts and peripheral blood mononuclear cells. Cell Physiol Biochem 2018; 47: 201-211.
[18] Saito T, Uchiumi T, Yagi M, Amamoto R, Setoyama D, Matsushima Y and Kang D. Cardiomyocyte-specific loss of mitochondrial p32/C1qbp causes cardiomyopathy and activates stress responses. Cardiovasc Res 2017; 113: 1173-1185.
[19] Schindl M, Függer R, Götzinger P, Längle F, Zitt M, Stättner S, Kornprat P, Sahora K, Hlauschek D and Gnant M. Randomized clinical trial of the effect of a fibrin sealant patch on pancreatic fistula formation after pancreatoduodenectomy. Br J Surg 2018; 105: 811-819.
[20] Tieftrunk E, Demir IE, Schorn S, Sargut M, Scheufele F, Calavrezos L, Schirren R, Friess H and Ceyhan GO. Pancreatic stump closure techniques and pancreatic fistula formation after distal pancreatectomy: meta-analysis and single-center experience. PLoS One 2018; 13: e0197553.
[21] Mizoguchi T, Ueno K, Yanagihara M, Samura M, Kurazumi H, Suzuki R, Morikage N and Hamano K. Autologous fibroblasts, peripheral blood mononuclear cells, and fibrin glue accelerate healing of refractory cutaneous ulcers in diabetic mice. Am J Transl Res 2018; 10: 2920-2928.
[22] Li X, Clappier C, Kleiter I and Heuchel R. Tamoxifen affects chronic pancreatitis-related fibrogenesis in an experimental mouse model: an effect beyond Cre recombination. FEBS Open Bio 2019; 9: 1756-1768.
[23] Young CC, Baker RM, Howlett CJ, Hryciw T, Herman JE, Higgs D, Gibbons R, Crawford H, Brown A and Pin CL. The loss of ATRX increases susceptibility to pancreatic injury and oncogenic

KRAS in female but not male mice. Cell Mol Gastroenterol Hepatol 2019; 7: 93-113.

[24] Lee SH and Hong TH. Pancreatic parenchymal injection of ethanol and octreotide to induce focal pancreatic fibrosis in rats: strategies to eliminate postoperative pancreatic fistula. Hepatobiliary Pancreat Dis Int 2018; 17: 81-85.

[25] Wang S, Zhang K, Hu JL, Wu WC, Liu X, Ge N, Guo JT, Wang GX and Sun SY. Endoscopic resection of the pancreatic tail and subsequent wound healing mechanisms in a porcine model. World J Gastroenterol 2019; 25: 2623-2635.

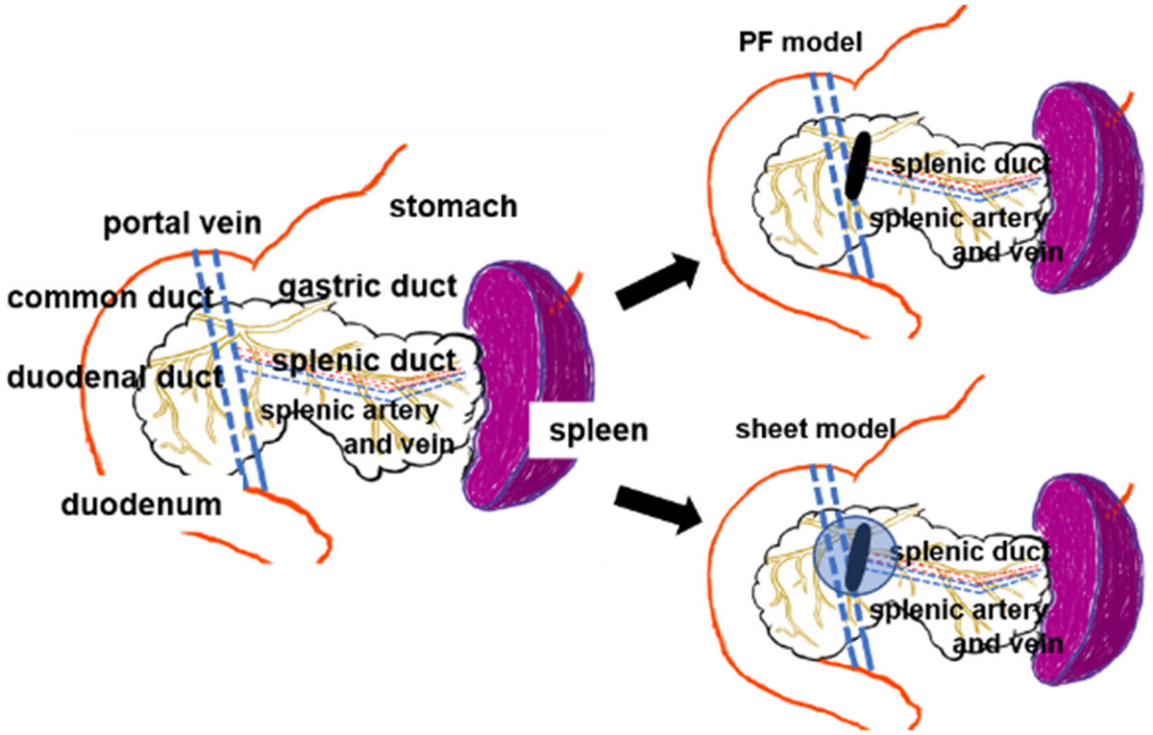

Supplementary Figure 1. Schema ilustration of rat pancreas and production of PF and sheet model. The rat pancreatic ducts consist of 4 ducts, e.g. common duct, gastric duct, duodenal duct, and splenic duct. The pancreatic fistula (PF) model was developed by the transection of the splenic duct and surrounding pancreatic parenchyma (at the left margin of the portal vein) with the preservation of the splenic artery and vein. The resection site is indicated by a black ellipse. The sheet models were developed by the transplantation of viable sheets, non-viable sheets or Seplafilm to the transection site.

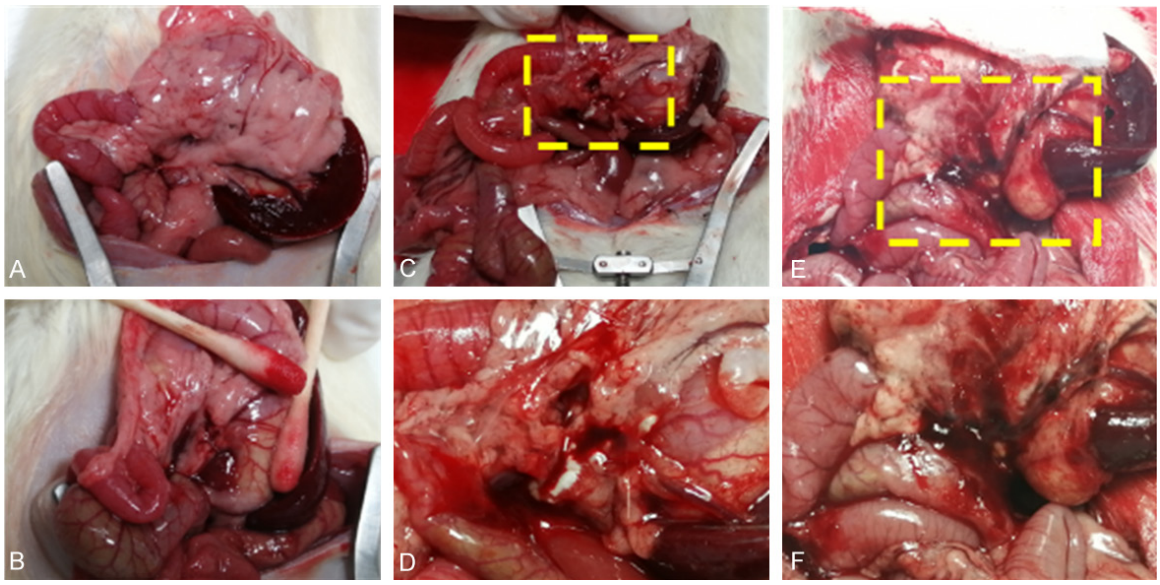

Supplementary Figure 2. Macroscopic findings in the abdominal organs before and after the transection of pancreas. (A) Abdominal findings after laparotomy without transection of pancreas. (B) Findings immediately after the transection of the splenic duct and surrounding pancreatic parenchyma. (C) Findings on POD 1. Strong inflammation with a small amount of ascites was observed. (D) A higher magnification of the demarcated area in (C). (E) Findings on POD 3. While inflammation remained, ascites had disappeared. (F) A higher magnification of the demarcated area in (@). Transection site was covered with hematoma.

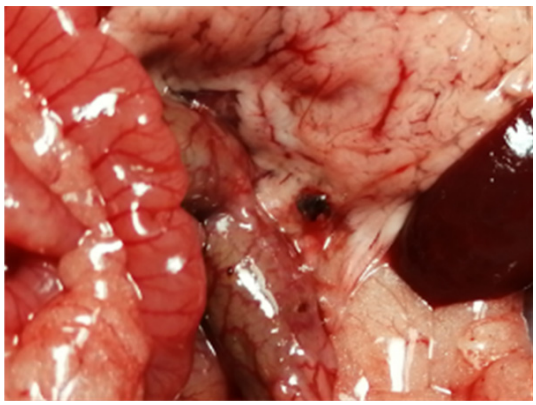

Supplementary Figure 3. Macroscopic findings in the abdominal organs in the PF model treated with the viable sheet. Inflammation was suppressed compared to those in the PF model on POD 1 (shown in Supplementary Figure 2C and 2D).

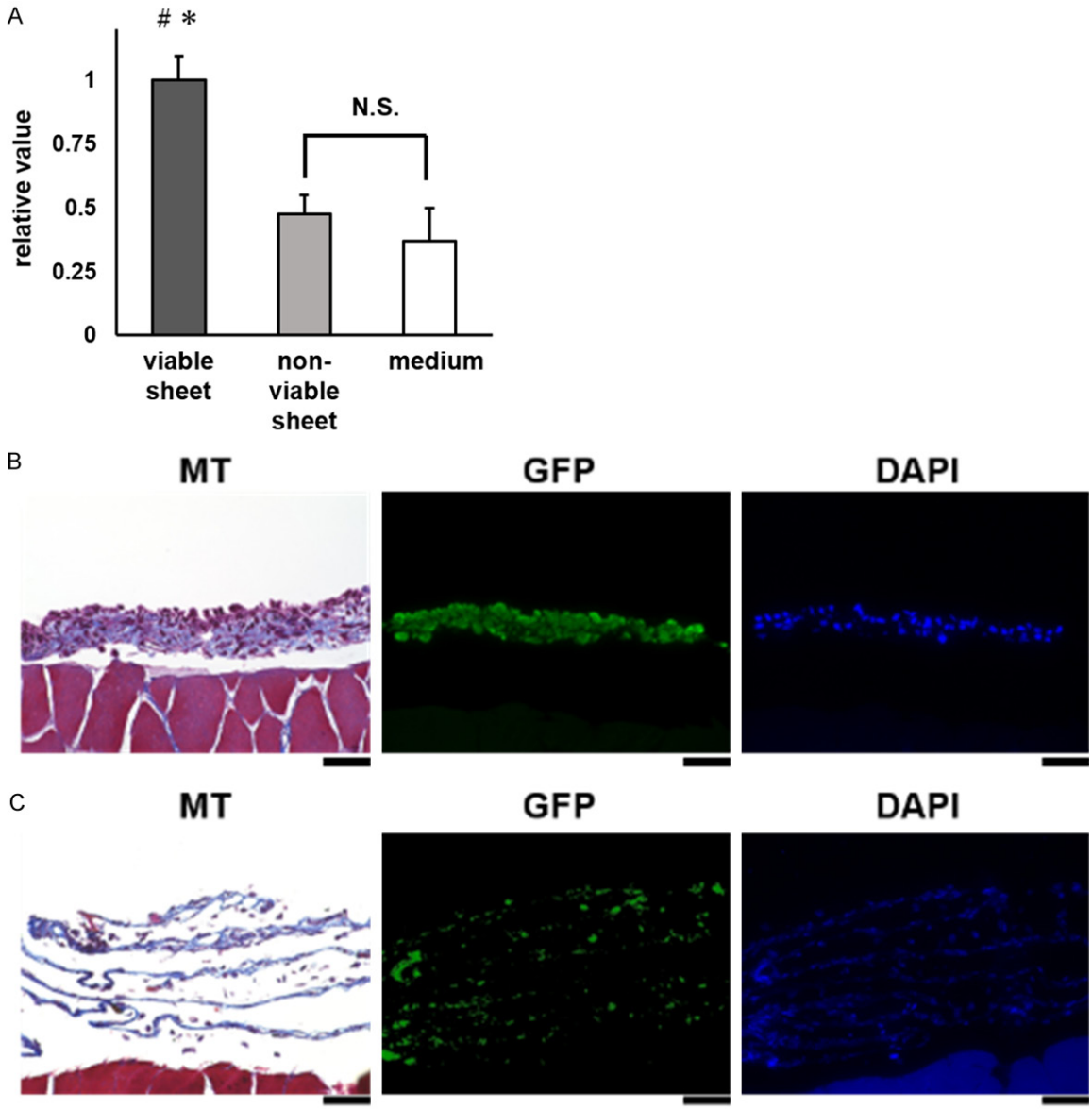

Supplementary Figure 4. Loss of cellular viability in non-viable sheet. A. Cellular viability was assayed with Cell Count Reagent SF in accordance with manufacturer's instructions. The value obtained with the non-viable sheet is comparable to that with medium alone, suggesting the loss of cellular viability in the non-viable sheet (n=3). #P<0.01 versus non-viable sheet, *P<0.01 versus medium, N.S. not significant (unpaired Student's t-test). B. Immunohistochemistry of mutilayered fibroblast sheets (viable sheet) prepared from the SD-Tg (CAG-eGFP) rat ubiquitously expresses enhanced green fluorescent protein (eGFP). Representative images of Masson's Trichrome (MT), GFP and DAPI stains are shown (scale bar, 50 um). The GFP signal was successfully detected. C. Immunohistochemistry of multilayered cytoskeleton sheets (non-viable sheet) prepared from SD-Tg (CAG-eGFP) rat. Representative images of Masson's Trichrome (MT), GFP and DAPI stains are shown (scale bar, 50 um). The GFP signal was almost abolished, indicating the protein degradation and loss of viability.

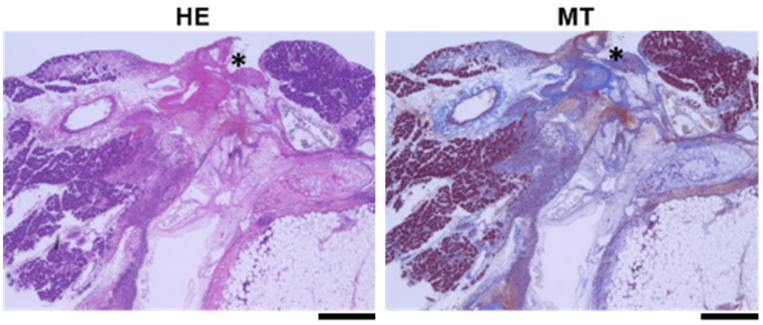

Supplementary Figure 5. Histologlcal analyses regarding the effect of the non-vlable sheet. The non-viable sheet only partially suppressed the necrosis and rescued fewer islets than the viable sheet (shown in **Figure 4A**). Representative images of Hematoxylin and Eosin (HE), Masson's Trichrome (MT) are shown (scale bar, 200 um). The asterisk indicates the transection site.

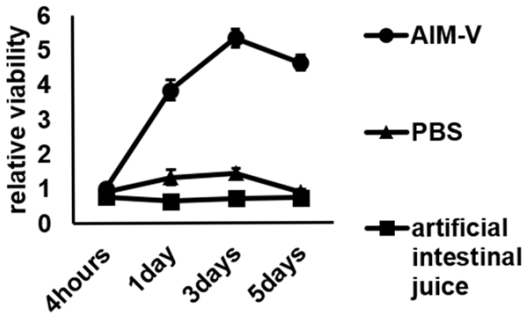

Supplementary Figure 6. The viability of cultured fibroblasts was seriously impaired in the presence of artificial intestinal juice or nutrient deficiency. The fibroblasts were initially plated at 5.0 × 10^4 cells/ml in a 96-well plate. After 2 h, the cellular adherence was confirmed, and the medium was replaced with phosphate-buffered saline or artificial intestinal juice. The viability was assayed with Cell Count Reagent SF after 4 h, 1 day, 3 days, and 5 days of culture (n=3). Pancreatin (FUJIFILM Wako Pure Chemical Corporation), which includes artificial amylase, proteases, trypsin and lipase, was diluted at pH 8.3 and used as atificial intestinal juice.